

Virtual Prototyping of Measurement Setup for Complex Light Scattering Properties

Vadim Sokolov¹, Igor Potemin¹, Dmitry Zhdanov¹, Sergey Pozdnyakov² and Alexey Voloboy²

¹ ITMO University, Kronverksky Pr. 49, St. Petersburg, 197101, Russia

² Keldysh Institute of Applied Mathematics RAS, Miusskaya sq. 4, Moscow, 125047, Russia

Abstract

The objects with complex light scattering, for example, light guiding plates with surface and volume microstructures are widely used in modern optical devices and computer graphics. Typically, such properties are described with Bi-Directional Scattering Distribution Function (BSDF) which totally describes the dependence of scattering properties on illumination and observation conditions. The precise BSDF measurements require complex setups with high resolution and launching numerous measurements in the entire angular space. The virtual prototyping of BSDF measurement devices is a difficult and problematic task because of the very small efficiency of similar systems. In the given paper the optimal and more effective ways to simulate such devices are presented based on example of patented scheme for portable BSDF measurements setup, including tolerance calculation and accuracy estimation.

Keywords

Light scattering, Bi-Directional Scattering Distribution Function, BSDF, BSDF measurements, virtual prototyping.

1. Introduction

The measurement of bi-directional scattering distribution function (BSDF) is one of the main ways to define complex light scattering properties of scattering objects like surfaces with microroughness, films, coatings with volume microstructures (paints, inks), etc. [1-4]. In many cases BSDF can be used directly in optical simulation and another cases it is necessary as additional data to obtain parameters of scattering objects, as an example parameters of volume microstructures. A variety of different BSDF measurement setups are presented in the modern market [5-11]. Besides, nowadays their development is being actively carried out. Thus, virtual prototyping of BSDF measurement devices to define light scattering properties of optical elements with scattering microstructures or to design BSDF measurement devices themselves to determine the proper parameters of their components, calculate tolerances, and evaluate measurement accuracy is the important task and the main goal of investigation in the given paper. The problems related to simulation of BSDF measurements setup are considered on the realistic example of precise, universal, portative optical device scheme.

Note that BSDF has a number of peculiarities, which complicates its measurements and simulation of setups aimed for BSDF measurements. First it is a multidimensional function. In general case four angles are required to define direction of illumination and observation plus color (wavelength), thus it is five parameters in sum, see figure 1a. Also, BSDF has two components: BRDF – bi-directional reflectance distribution function and BTDF – bi-directional transmittance distribution function and they can be different from different side of scattering elements, see figure 1b. Another peculiarity is variation of light scattering properties. BSDF samples can be very dark, or in opposite very bright, they can have properties close to diffuse or close to mirrors, automotive paints can have very complex angular and spectral distributions depending on observation and illumination conditions.

GraphiCon 2023: 33rd International Conference on Computer Graphics and Vision, September 19-21, 2023

V.A. Trapeznikov Institute of Control Sciences of Russian Academy of Sciences, Moscow, Russia

EMAIL: sokolovv1969@gmail.com (V. Sokolov); potemin@yandex.ru (I. Potemin); ddzhdanov@mail.ru (D. Zhdanov); mephi32@rambler.ru (S. Pozdnyakov); voloboy@gin.keldysh.ru (A. Voloboy)

ORCID: 0000-0002-1719-5102 (V. Sokolov); 0000-0002-5785-7465 (I. Potemin); 0000-0001-7346-8155 (D. Zhdanov); 0000-0003-2090-8035 (S. Pozdnyakov); 0000-0003-1252-8294 (A. Voloboy)



© 2023 Copyright for this paper by its authors.

Use permitted under Creative Commons License Attribution 4.0 International (CC BY 4.0).

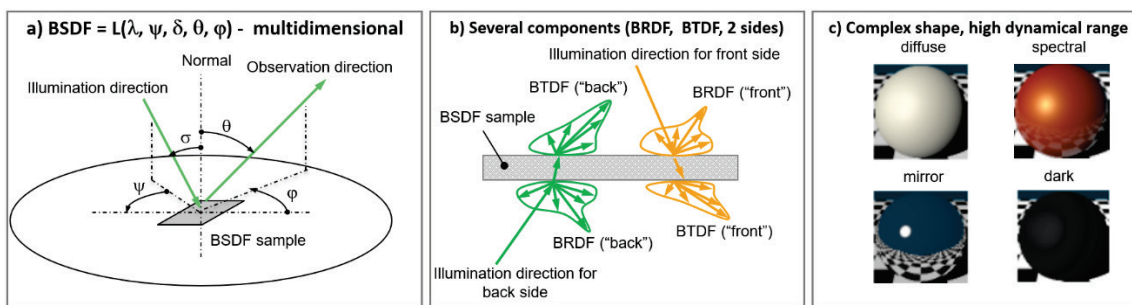


Figure 1: BSGF peculiarities

BSGF measurement setup should launch a lot of measurements directions to cover all angular space for both illumination and observation from both sides of sample to be measured. BSGF shape can be very complex, especially in the case of samples with properties close to specular, so accurate measurements require very high resolution of sensors detecting light scattered and very detailed angular grid for observation directions at least. It complicates optical schemes of BSGF measurements setups with a lot of movable units. Apart from such models have very small efficiency, because only very small part of scattered light flux is detected by device sensors relative to total light flux emitted with device light source. Also, the evaluation of tolerances for device units requires many calculations for a lot of different parameters configuration. At last, a stochastic ray tracing is applied to calculate optical schemes with scattering elements and these approaches require long calculation time. All mentioned problems extremely complicate effective virtual prototyping of similar devices. In this work the way to simulate the similar setups effectively is shown on example of optical scheme of patented BSGF measurement setup [12].

2. Measurement setup

Optical scheme of BSGF measurement setup is presented in figure 2.

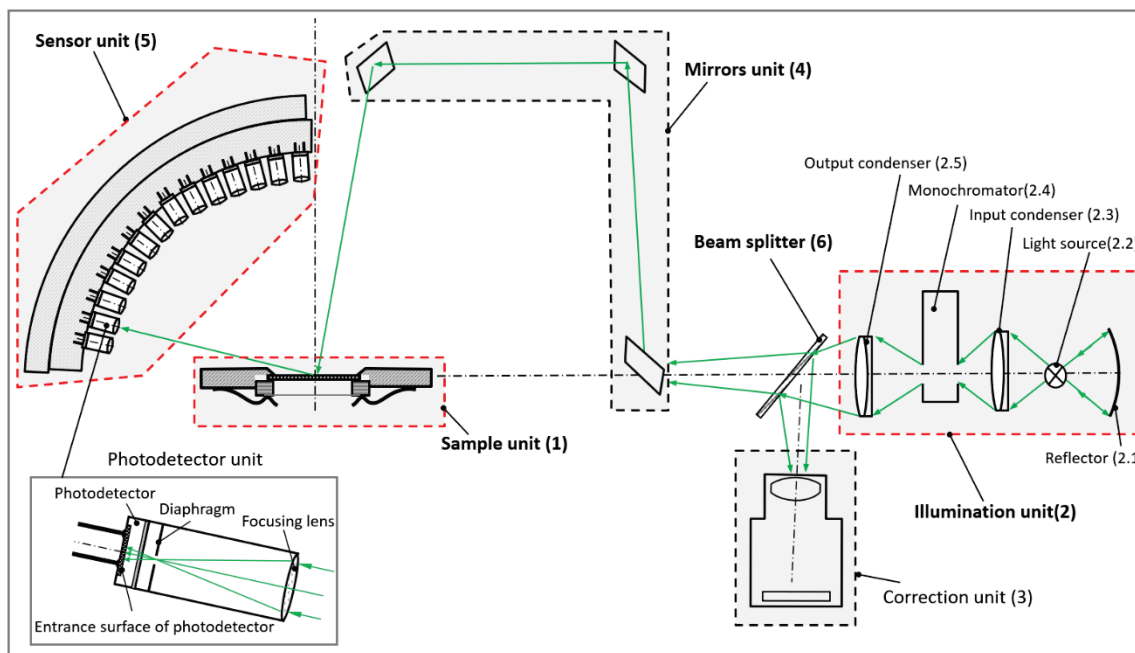


Figure 2: Optical scheme of BSGF measurement setup

First, the optical scheme of device contains three main units necessary for any setup measuring BSGF (marked with red contours). It is a sample unit, an illumination unit, and a sensor unit. The sample unit is aimed for measuring sample layout. The illumination unit generates a light beam close to parallel designed for sample illumination with monochrome collimated light beam. The sensor unit detects light

scattered by measured sample. It contains a set of units with photodetectors placed on a two-component quarter-circle arc. There are two additional units. A correction unit is used to control fluctuations of luminous flux emitted with the light source of the illumination unit and the mirror unit. The mirror unit is designed to modify incident direction of light. It contains three mirrors placed in three vertices of rectangle; in the fourth vertex of rectangle a measured sample is placed. The mirror unit is rotated around the optical axis of the illumination unit and modifies polar angle of sample illumination linearly.

The white light emitted with the light source of the illumination unit is projected with input condenser and reflector on monochromator entrance slit. The narrow spectral band light is projected from monochromator exit slit to the center of measuring sample by an output condenser. The part of light leaving the illumination unit is redirected to correction unit by beam splitter. And finally light scattered by the measuring sample is detected with the sensor unit.

The dynamics of the device are presented in figure 3.

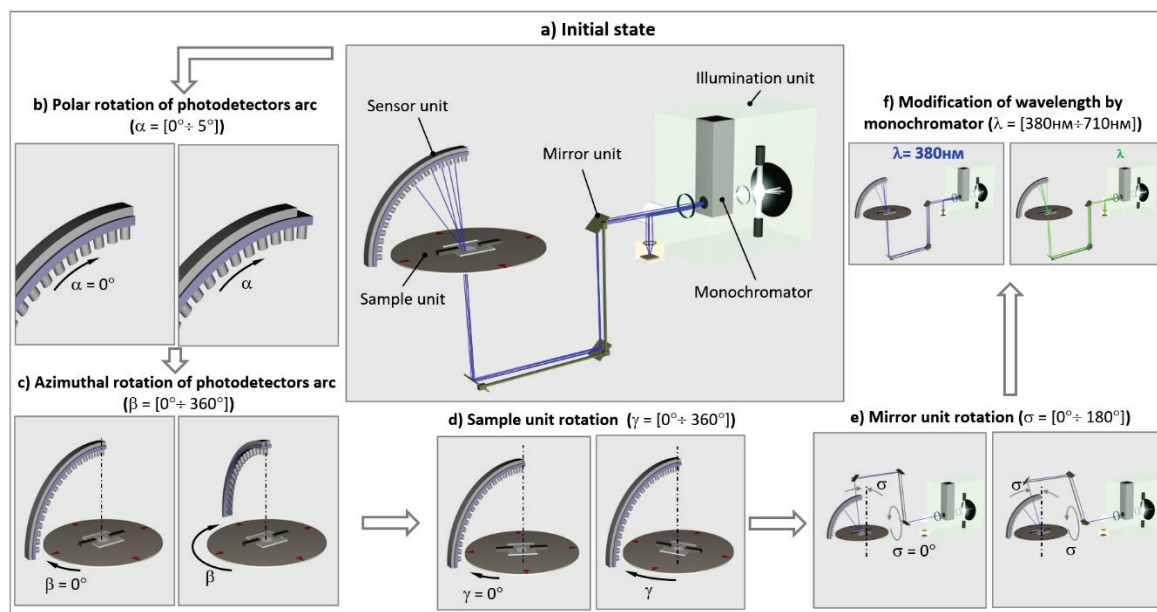


Figure 3: Dynamics of BSRF measurement setup

The central image (see figure 3a) presents optical scheme of the device in static with initial positioning of all units. Dynamics of separate units are presented on the images placed around of central image from the left to the right. A polar rotation of photodetector arc (see figure 3b) is launched for measurements with high angular resolution when the samples properties close to specular. On the next step azimuthal rotation of photodetectors around vertical axis on β angle is run to cover the entire angular space with measurements (see figure 3c). In the case of measurements of sample with isotropic scattering the range of β angle is from 0° to 180° and from 0° to 360° in case of anisotropic samples. The next two rotations are aimed for modification of illumination direction. The figure 3d shows rotation of sample unit around vertical axis on angle γ (from 0° to 360°). This rotation is necessary only in the case of anisotropic samples measurements. The rotation of mirror unit is presented in figure 3e. It modifies the polar angle σ of incident light. It varies from 0° to 90° for BRDF measurements and from 90° to 180° for BTDF measurements. The final step in measurement scheme is modification of wavelength with monochromator unit (see figure 3f). The wavelength varies in the visible range from 380 to 710nm.

Rather outstanding parameters have place in the device specification. The angular resolution of the device (photodetectors) is varied from 0.5° to 2.5° . The minimal angular step for all movable units is up to 0.1° . It means, that a very detailed angular grid can be specified for measured BSRF. The computer simulation of such a multiunit system is quite a complex task. The direct approaches to calculate consequentially all steps of layout modification of different device units explained above are not appropriate at all. Much more effective ways of acceleration for lighting calculation are considered in the next chapter.

3. Computer model

When developing computer models of devices for BSDF measurements, one should consider the fact that they usually contain elements (surfaces) with complex light scattering, in our case this is only a plane measured sample, in other schemes it can also be other elements such as diffuse reflectors of a spherical or more complex shape. In this case, rather complex algorithms of stochastic ray tracing are used for optical modeling. In addition, the photodetectors in devices for BSDF measurements have very small values of the angular and linear apertures to provide high resolution for BSDF measurements. The latter fact makes such systems extremely inefficient in terms of calculation speed, which can take a significant amount of time. These problems have been studied on computer models of real measuring systems, for example, in [13, 14]. These papers provide some guidance on how to simplify individual nodes as much as possible when modeling them, use multiple virtual detectors simultaneously, and apply optimal ray tracing techniques. These recommendations were used in the development of a computer model of the BSDF measurement setup.

3.1. Optical scheme

The general optical scheme for virtual prototype of BSDF measurement setup is shown in figure 4.

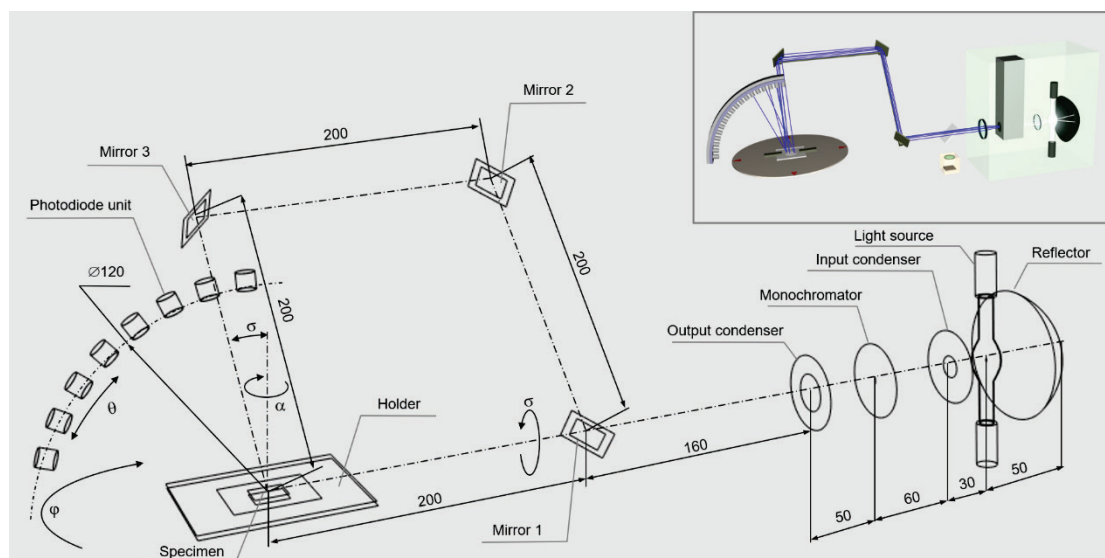


Figure 4: Scheme of a computer model

Comments to figure 4: All dimensions shown are in mm. The computer model includes the sample unit, illumination unit, three-mirror unit, and sensor unit. The correction unit declared in the real circuit of the device is designed to control fluctuations in the lamp radiation flux, which is irrelevant in the simulation, so this part of the device was excluded from the model.

The sample unit is represented in a simplified way by several elements - a rectangle (one-sheet flat surface) with properties to be measured by the setup and two rectangular frames placed above and below the sample with square holes. Their purpose is to fix the sample and limit the illumination area of the sample, which takes place in a real installation. The entire sample unit can be rotated around the vertical axis by an angle α to modify the azimuth of illumination direction.

The mirror unit is modeled by a simple set of three square one-sheet surfaces with mirror properties (mirrors 1, 2, 3 in figure 4). The distance between the mirrors and the sample is the same and equal to 200 mm. This distance was chosen to provide the divergence of the illuminating beam in the range of $0.5^\circ \div 1^\circ$. The mirror unit is rotated in the model by an angle σ around the lower side of the square containing the sample and mirror 1 and coinciding with the optical axis of the illumination unit to provide a smooth change of the polar angle of light incidence on the sample. The specular reflectance of the mirrors was set to 95%.

The illumination unit is represented by a light source, a reflector, an input condenser, a monochromator, and an output condenser. A xenon lamp model was chosen as the light source [15]. The model of the lamp is presented with the help of a glass bulb, cartridges, and the main object (effective arc size) – a self-luminous cylindrical body with a radius equal to 0.5 mm and a length of 2.2 mm. The emission spectrogram and the luminous flux were set in accordance with the specification provided by the manufacturer of the real lamp.

The spherical reflector has a radius of 50 mm. The center of reflector curvature is placed in the center of the luminous body of the lamp, respectively, the distance from the top of the reflector to the center of the effective arc is also 50 mm. The working surface of the lamp reflector has a specular reflectance equal to 95%.

All lenses in the device were simulated as ideal lenses to speed up calculation. This device does not belong to imaginary optics and does not need to accurately reproduce a real image, and thus this simplification is quite reasonable.

The monochromator is simulated in a simplified way using an opaque diaphragm with a rectangular slit, the size of which coincides with the entrance/exit slit of a real monochromator [16] and is equal to $4\text{mm} \div 0.5\text{mm}$. A rectangular slit is modeled by a transparent surface, the transmission wave interval of which can vary arbitrarily.

The model of the sensor unit was designed in two versions: closer to the "real" and simplified. In the "real" version, the detector units consist of ideal lenses (see 1 in figure 5a), a frame 2, a diaphragm 3 with a variable aperture diameter, and a light detector 4. The detectors are distributed along the round arc, their number is set by a grid of polar angles, there is an additional possibility of their polar and azimuthal rotation around the vertical axis.

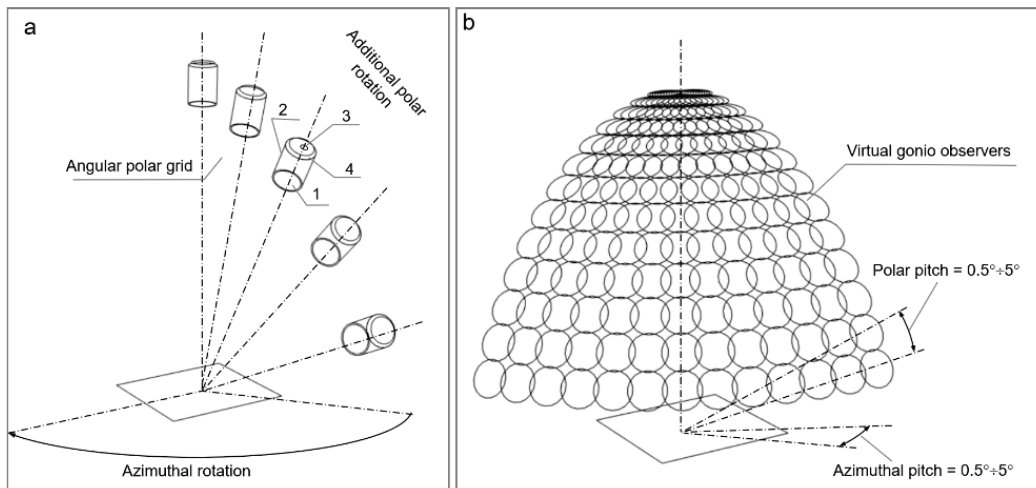


Figure 5: Variants of the sensor unit schemes: "real" (a), "simplified" (b)

However, the calculation of the entire BSDF based on such a sensor unit model with gradual azimuthal rotations and polar shifts in the case of using a high resolution is inefficient. So, the "real" model was used only for testing. To calculate BSDF on a detailed angular grid, a simplified model was created (see figure 5b). In this version, the sensor unit is represented by a set of virtual detectors (observers), circles with a diameter of 5 mm and an angular resolution corresponding to real detectors with lenses, which can vary in the range of $0.5^\circ \div 2.5^\circ$. These detectors do not affect the light propagation in the system and can be set in any number with an arbitrary angular step in both azimuthal and polar directions, their intersection does not affect the propagation of scattered light either, thus it is possible to calculate all directions of observation simultaneously when using the camera independent ray tracers. For BSDF measurements simulation the step between the detectors varied from 0.5° in directions close to specular to 5° in diffuse directions. Note for better visualization in figure 5, a reduced number of detectors is shown.

3.2. BSDF calculation in computer model

BSDF calculation itself does not pose a problem in the presence of known luminances (or light fluxes) of the sample and the diffuse etalon accumulated with virtual detectors of computer model and can be defined as the ratio of these luminances for specific directions of observation, illumination, and wavelength, see formula 1.

$$BSDF(\lambda, \Psi, \delta, \varphi, \theta) = \frac{F_{sample}(\lambda, \Psi, \delta, \varphi, \theta)}{F_{etalon}(\lambda, \Psi, \delta, \varphi, \theta)} BSDF_{etalon}(\lambda, \Psi, \delta, \varphi, \theta) \quad (1)$$

Where $BSDF(\lambda, \Psi, \delta, \varphi, \theta)$ is value of luminance factor of measured sample for given $\lambda, \Psi, \delta, \varphi, \theta$, see figure 1. Its distribution defines BSDF of sample. F_{sample} is luminous flux of scattered light detected with device detector, F_{etalon} is luminous flux emitted with etalon (standard) and $BSDF_{etalon}$. In the given model it is equal to 1 for all angles and wavelengths because ideal Lambertian properties are used in computer model.

To speed up the calculation process, it is important to choose the optimal calculation method. The stochastic forward Monte Carlo ray tracing engine available in the Lumicept software package [17] was chosen. The Monte Carlo method of direct stochastic ray tracing is not the fastest calculation method, more complex and efficient combined methods for calculating scattered light have been developed, combining both direct ray tracing methods (tracing starts from the light source) and reverse (from observer), however, these methods are usually dependent on the camera (the sensor position). In the case of a computer model of the device, it is required to calculate many detectors, and it is desirable to calculate them simultaneously, that forward stochastic ray tracing by the Monte Carlo method allows.

Another task in BSDF calculation is to bring its coordinate system to the required type. In the computer model, the position of the detector is determined in the usual geocentric coordinate system, where the direction of observation is determined by two angles: α azimuth and β polar (elevation). However, in the case of Lumicept [17], BSDF is defined in a different coordinate system. It is shown in figure 6, where BRDF is defined with respect to the specularly reflected beam in the case of BRDF and the refracted beam in the case of the BTDF, where the direction of observation is specified with angles θ and φ . The angle θ is the angle between the direction of the specular reflection \vec{r} and the direction of observation \vec{d} , and φ specifies the rotation of the direction of observation around the direction of the specular reflection. Thus, data calculated in the original geocentric coordinate system of computer model (angles α, β) must be converted to σ, θ, φ .

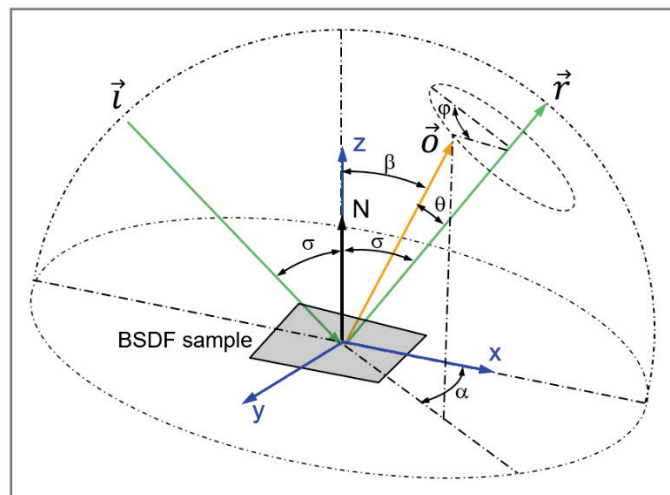


Figure 6: BSDF coordinate system defined with respect to the specularly reflected beam. \vec{l} , - direction of light incidence, \vec{r} , - direction of reflection of light, \vec{d} , - direction of observation

From figure 6, α, β angles can be determined with known (o_x, o_y, o_z) ords of the observation vector \vec{d} according to formula 2:

$$\alpha = \arctg 2 \left(\frac{o_x}{o_y} \right); \beta = \frac{\sqrt{o_x^2 + o_y^2}}{|\vec{d}|} \quad (2)$$

The orts of the vector \vec{d} are easy to derive for the case of normal sample illumination at an angle $\sigma = 0^\circ$, see formula 3:

$$o'_x = \cos(\theta); o'_y = \sin(\theta)\sin(\varphi); o'_z = \sin(\theta)\cos(\varphi) \quad (3)$$

By rotating the system by the required angle σ , the required values of the orts of the observation vector \vec{d} can be derived, see formula 4:

$$\begin{bmatrix} o_x \\ o_y \\ o_z \end{bmatrix} = \begin{bmatrix} \cos(\sigma) & 0 & -\sin(\sigma) \\ 0 & 1 & 0 \\ \sin(\sigma) & 0 & \cos(\sigma) \end{bmatrix} \times \begin{bmatrix} o'_x \\ o'_y \\ o'_z \end{bmatrix} \quad (4)$$

From formulas (2) and (4), it is possible to determine the angles α and β as functions of θ , φ and σ and convert calculated BSDF to required angular grid. Finally, the BSDF calculation scheme used in the computer model is shown in figure 7.

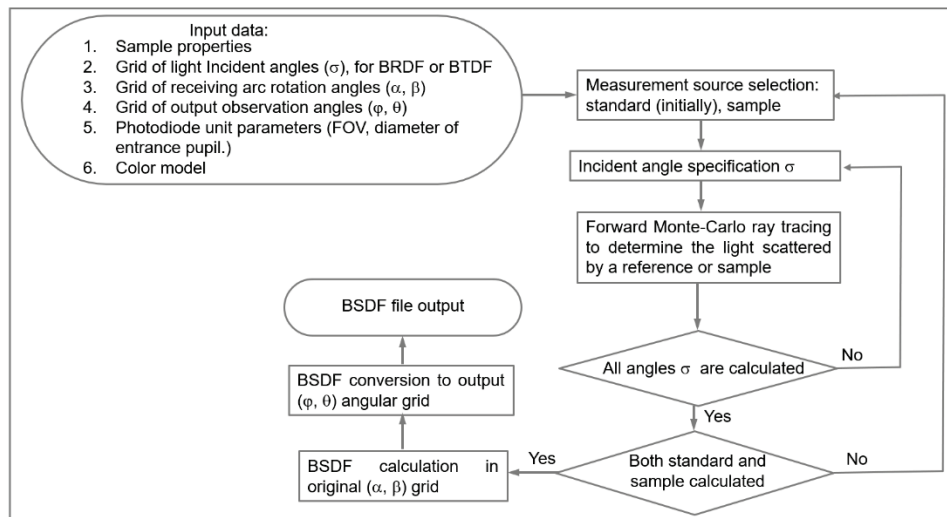


Figure 7: Scheme of BSDF calculations in a computer model

To calculate BSDF on the sample surface scattering properties in interest are specified, for example, a theoretical BSDF with a known shape. In addition, a grid of incident angles σ is set to determine the lighting conditions of the sample, a grid of angles α , β (see figure 6), which defines a complete set of positions of virtual detectors. To generate BSDF output file, a grid of angles φ , θ should be specified too. The developed model makes it possible to calculate BSDF both in grayscale and spectral format. Ideally, to launch spectral calculations, in accordance with the developed scheme, it is necessary to sequentially calculate light scattering for a set of beams with different wavelengths, which can be set using a monochromator. To speed up the calculation when determining the entire BSDF, the sample is illuminated with the full spectrum in range 380nm-780nm. Such a simplification is quite justified when sample does not have fluorescent properties.

First, properties of the diffuse etalon (sample with Lambertian BSDF) are set for a surface emulating measured sample in the model. The position of the mirror unit is set according to the initial angle σ , and detectors - accordance to the grids of angles α and β (see figure 6). Then Monte Carlo ray tracing is run to calculate light scattering. The calculations are repeated for all σ angles with corresponding rotation of mirror unit. After performing all calculations for the standard, the same procedure is repeated for scattering properties of sample in interest. Further, the luminous fluxes detected from the sample and the standard are recalculated into the distribution of luminance factor (= BSDF see formula 1). Finally, it is converted to the output grid of angles σ , φ , θ with storing into BSDF file of Lumicept format.

3.3. Tolerances calculation

Any BSDF measurement setup is a complex optical system with a large set of moving elements, the deviation of the parameters of which can have a significant effect on the accuracy of BSDF measurements. The evaluation of tolerances in such a device involves the implementation of numerous calculations (thousands) necessary to determine their complex influence on the accuracy. It should also be noted that even considering all the simplifications that were made in the developed computer model, the calculation of one BSDF takes a significant amount of time (hours), and it is not acceptable in case of tolerances estimations. To solve this problem, the decomposition of the model is used, namely, the illumination unit is simulated separately. The goal of the unit is to illuminate sample with light beam close to parallel. The main characteristic of the unit is the value and uniformity of illumination created on the sample surface and angular divergence of illumination beam, see figure 8.

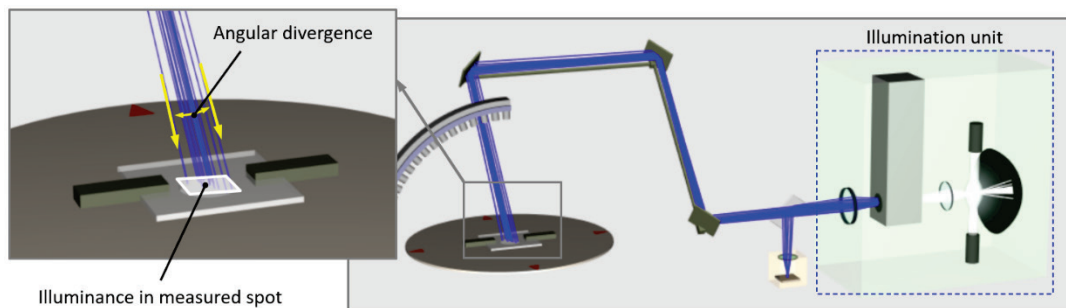


Figure 8: Main output characteristics of illumination unit

The angular divergence is determined to a greater extent by the distance between the exit pupil of the illumination unit and the sample surface, which is almost impossible to influence without a fundamental change in the device scheme. The main deviations of the elements of the illumination unit are shown in figure 9. These are the angular and spatial deviations of the entire illumination unit and its parts. All these deviations were used in the tolerance estimation.

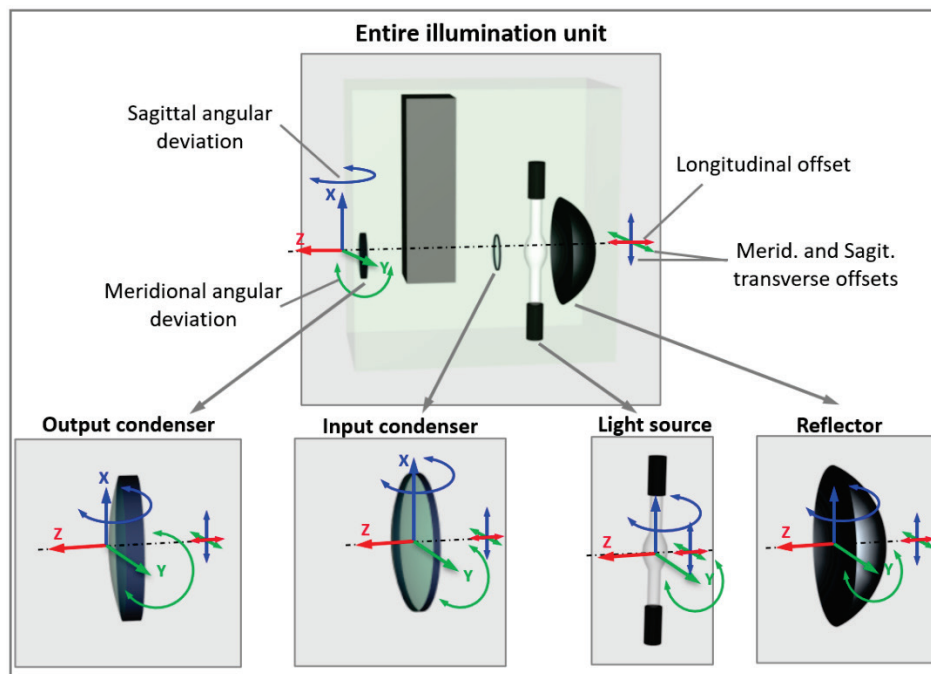


Figure 9: Deviations of the illumination unit elements

Tolerances were calculated based on the condition that the luminous flux incident on the sample is located in the center of the sample and has sizes not less than 5 mm ÷ 5 mm does not differ by more than 5–10% from the value calculated for zero deviations.

The tolerances were calculated according to the following algorithm: at the initial step, the permissible deviation ranges for each individual parameter were determined, all other deviations were set to zero. After determining the permissible limits for each individual parameter, their mutual influence was assessed. To solve the last problem, a set of possible values was formed for each deviation within its allowable values with a certain step. Further, calculations were made for all possible combinations of deviations of all parameters (“brute force” optimization). Based on the analysis of the calculated variants, all that gave an unacceptable output result were removed and the tolerances were recalculated, already considering the mutual influence of deviations. For the illumination unit, permissible angular and spatial deviations are presented in table 1.

Table 1: Permissible deviations of illumination units elements positioning

Angular deviations	Spatial deviations
±0.05°	±0.025mm

Note only minimal values for permissible deviations are presented in table 1. Mainly it is related to positioning of reflector, entire illumination unit and output condenser. The tolerances for other elements are rougher. In all further calculations, in order to speed up the calculation when simulating the entire device, the illumination unit was replaced by a rayset light source. The rays emitted with illumination unit were recorded for worst combination of deviations of its parts. The final model of the entire device is shown in figure 10.

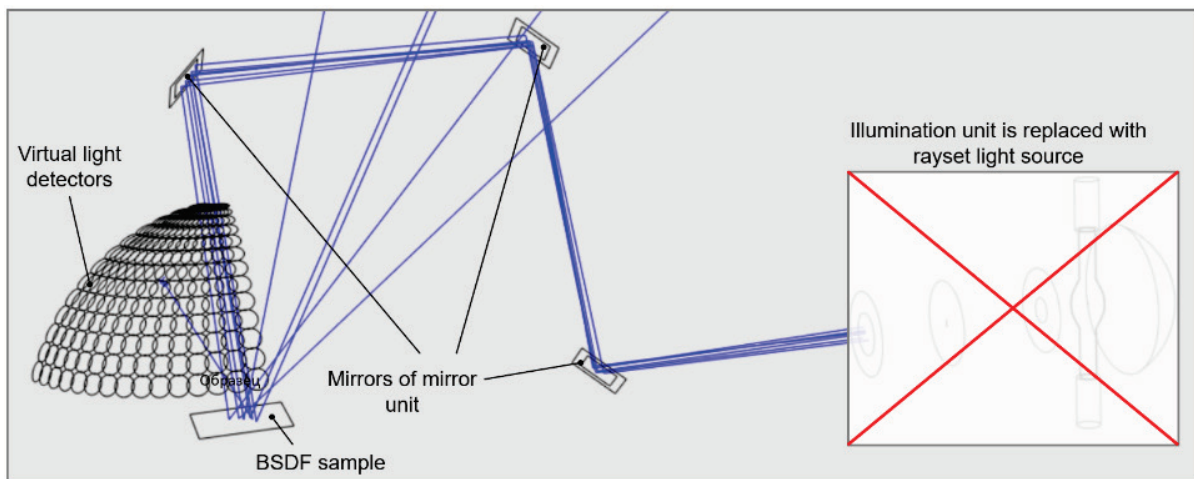


Figure 10: The final computer model of the device with a rayset light source

The main errors of BSDF measurements which can be introduced with angular positioning deviations of the sample unit. It is divided into two orthogonal components, meridional and sagittal angular deviations. Similar deviations are possible in each mirror of mirror unit and in the positioning of sensor unit photodetectors, as it is presented in figure 11.

The calculation of tolerances was carried out similarly to the calculation of the tolerances of the illumination unit, only with the different output, instead of the sample illumination, the deviation in BSDF from theoretical Gaussian-shaped BSDF with a 5° angular width is used. It is explained in more detail in the next chapter. The error between the theoretical and calculated BSDF is determined by the relative standard deviation (relative RMS), see formula 5 and should not exceed 5%.

$$RMS_{relative} = \sqrt{\frac{\sum_i \left(\frac{L_{si} - L_{ti}}{0.5(L_{si} + L_{ti})} \right)^2}{n}} * 100\% \tag{5}$$

where L_{si} is a BSDF value (luminance factor) simulated with computer model and L_{ti} – a value of theoretical Gaussian BSDF, i index determines direction of observation and illumination.

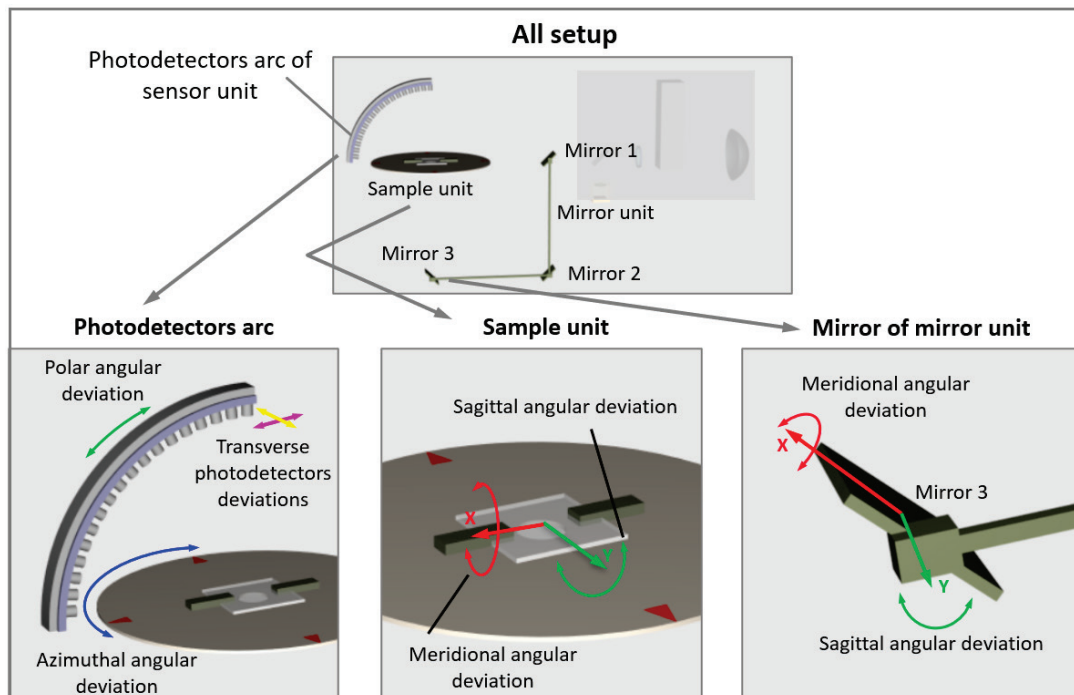


Figure 11: Main deviations in sample, mirror, and sensor blocks

Table 2 presents permissible angular and spatial deviations for the worst-case scenario of their combinations, like table 1.

Table 2: Permissible deviations for elements of sample, mirror and sensor units

Angular deviations	Spatial deviations
$\pm 0.05^\circ$	$\pm 0.1\text{mm}$

It should be noted that the permissible values presented in tables 1 and 2 show that they are not sufficiently rigid in terms of the possibility of manufacturing the device. Graphical information on the results of tolerance evaluation is presented in the next chapter.

4. Simulation results. Accuracy estimation

To test the developed model, the analytical "Gaussian" BSDF was chosen. It defines intensity distribution, according to formula 6.

$$I(\theta) = I_o \exp\left(-\left(\frac{\theta}{\alpha}\right)^2\right) \tag{6}$$

where θ is an angle between the directions of observation and specular reflection or transmission. α is an angular width (the angle at which intensity is halved relative to the intensity I_o in specular direction). The four variants of Gaussian BSDF have been selected for investigation with angular width = $0^\circ, 5^\circ, 15^\circ$ and 30° , see figure 12.

Figure 13 presents graphs comparing BSDFs obtained from simulations with their theoretical counterparts. All simulations are carried out here for the minimal angular field of view of photodiode unit equal to 0.5° . The graphs show the distribution of the luminance factor given for three illumination angles $\sigma = 0^\circ$ (red), 30° (yellow), 60° (green) in the plane of light incidence. The solid line marks the theoretical BSDFs, the dotted line marks BSDF calculated using the computer model. Note all simulations have been launched with the worse combination of deviations for all device elements (subject to tolerances).

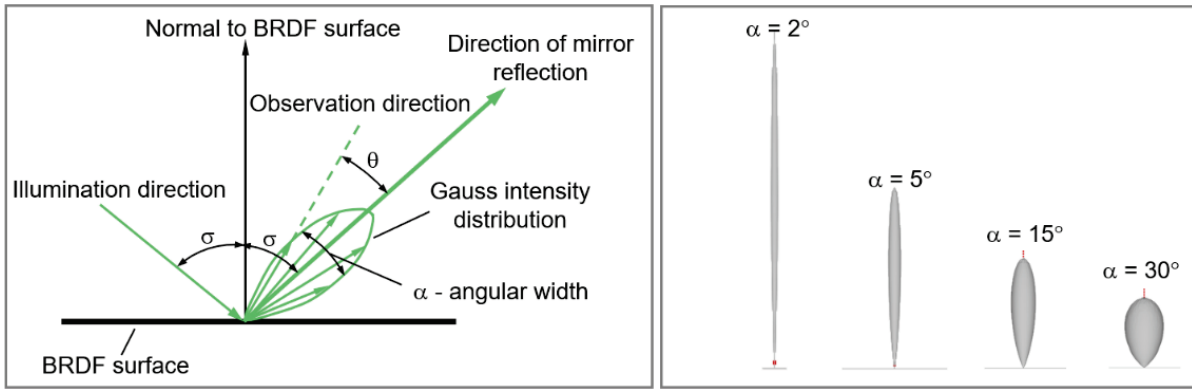


Figure 12: Gaussian distribution in dependence on α (“angular width”) value

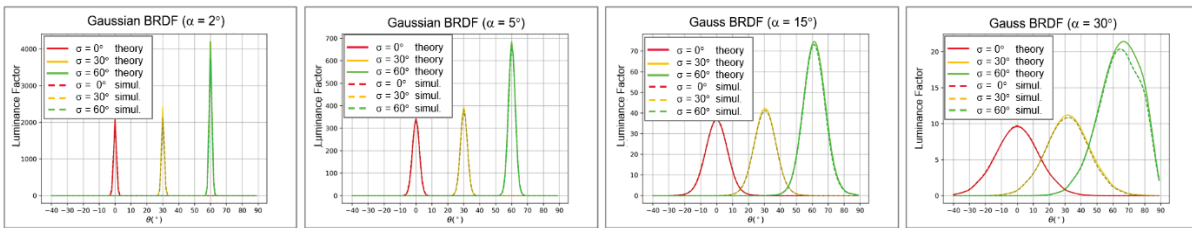


Figure 13: Comparison of analytical (theoretical) BRDF with simulated ones

The numerical results of modeling the "Gaussian" BSDF are presented in table 3

Table 3: Deviations between simulated and analytical BRDF

Light incident angle	Gaussian angular width α			
	$\alpha = 2^\circ$	$\alpha = 5^\circ$	$\alpha = 15^\circ$	$\alpha = 30^\circ$
$\sigma = 0^\circ$	4.79%	2.74%	0.37%	0.20%
$\sigma = 30^\circ$	4.21%	1.90%	0.56%	0.47%
$\sigma = 60^\circ$	3.85%	1.83%	0.74%	0.63%

Note deviations in table 3 are calculated as relative RMS between expected (theoretical) BRDF and BRDF simulated with computer model, see formula 7.

For a visual representation of the simulated "Gaussian" BRDF, images of a sphere placed in a cube with checkerboard faces and illuminated by a rectangular light source were synthesized, see figure 14. The first row shows images synthesized for a sphere with a theoretical BRDF, the second – simulated with computer model. Only variants considering tolerances are shown. Visual evaluation from the images presented in figure 14 shows an almost perfect similarity between the images synthesized based on the target theoretical BRDF versus their counterparts calculated using the computer model of the measuring device. The images were synthesized with advanced “Path Tracing” lighting engine available in Lumicest [17].

5. Conclusions

The model of BSDF measurements setup presented in the paper is extremely complex from viewpoint of virtual prototyping because of its small lighting efficiency. Direct approaches to simulate the similar models will takes hours for BSDF calculation what does not allow to use them in numerous simulations requiring estimating tolerances or optimization procedures used for reconstruction of parameters of complex scattering materials. The techniques used in this study for computer simulation, such as the choice of the optimal ray tracer (forward Monte-Carlo ray tracing) that allows to simulate all directions of observation simultaneously, as well as the decomposition of the model (replacing the illumination unit with a rayset light source), can greatly speed up the calculation process and launch necessary virtual prototyping effectively.

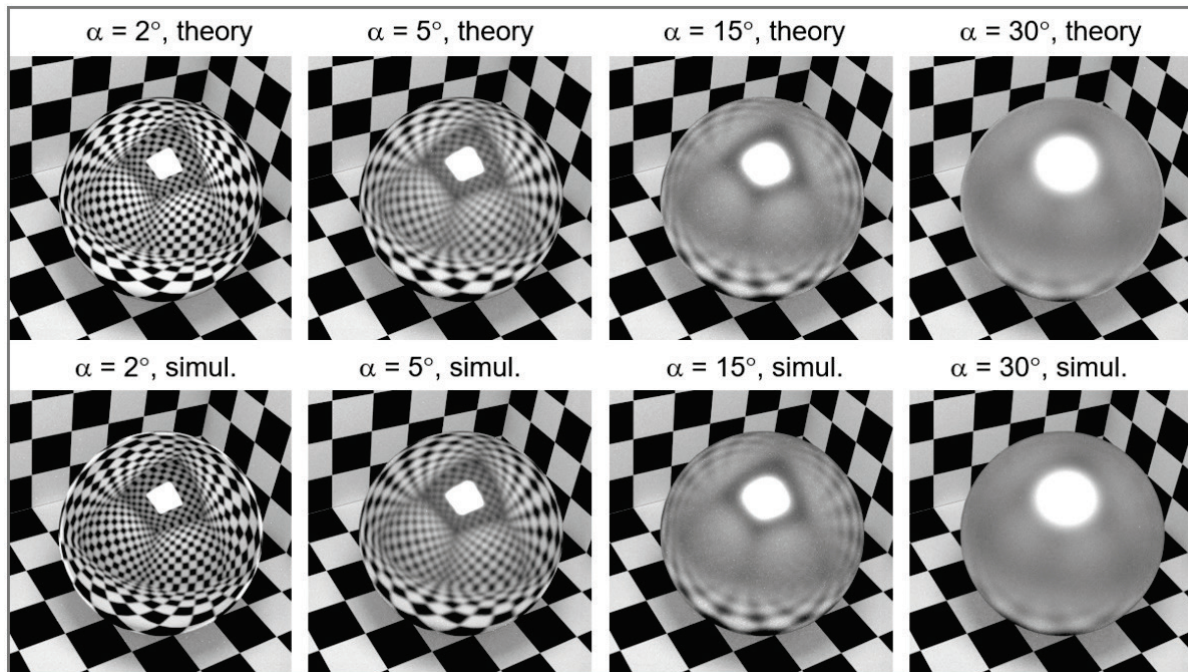


Figure 14: Visual comparison of analytical (theoretical) BRDF with simulated ones

6. Acknowledgements

This work was supported by the Russian Science Foundation, project no. 22-11-00145.

7. References

- [1] F. O. Bartell, E. L. Dereniak, and W. L. Wolfe, "The Theory And Measurement Of Bidirectional Reflectance Distribution Function (BRDF) And Bidirectional Transmittance Distribution Function (BTDF)," Proc. SPIE 0257, Radiation Scattering in Optical Systems, (3 March 1981). <https://doi.org/10.1117/12.959611>.
- [2] K. Torrance and E. Sparrow. Theory for Off-Specular Reflection from Roughened Surfaces. J. Optical Soc. America, vol. 57., pp. 1105—1114, 1976.
- [3] Ward, J. Gregory "Measuring and modeling anisotropic reflection". Proceedings of SIGGRAPH. (1992), pp. 265—272. doi:10.1145/133994.134078.
- [4] James F. Blinn. Models of light reflection for computer synthesized pictures // Proc. 4th annual conference on computer graphics and interactive techniques: journal. 1977. pp. 192. doi:10.1145/563858.563893.
- [5] X-Rite MA98 Portable Multi-Angle Spectrophotometers, X-Rite, 2023. URL: https://www.tricolor.pl/images/pdf/L10-372_MA98_en.pdf.
- [6] MA-T12 Handheld Multi-Angle Spectrophotometer | X-Rite 12-Angle Color Measurement, X-Rite, 2023. URL: <https://www.xrite.com/categories/portable-spectrophotometers/ma-family/ma-t12>.
- [7] Optical Scattering Measurement & Equipment | Synopsys, Synopsys Mini-Diff VPro, SYNOPSIS, 2023. URL: <https://www.synopsys.com/optical-solutions/scattering-measurements.html#MiniDiffVPRO>.
- [8] Imaging Sphere for Scatter and Appearance Measurement IS-SA, Radiant Vision Systems, 2022. URL: <https://sphereoptics.de/wp-content/uploads/2014/03/Radiant-ImagingSphere-IS-SA.pdf>
- [9] Ansys Optical Measurement Device Solutions, ANSYS AMO-PRO, AMO-Premium, Ansys, 2023. URL: <https://www.ansys.com/content/dam/product/optical/omd/ansys-omd-technical-description-sheet.pdf>.

- [10] Gonio Photometer GP-700 | Murakami Color Research Laboratory, Murakami Color Research Laboratory, 2023. URL: https://www.mcrcl.co.jp/english/products/p_color_sp/detail/GP700.html
- [11] Gonio-Spectrophotometric Color Measurement System GCMS-4B, 2023. URL: https://www.mcrcl.co.jp/english/products/p_color_sp/detail/GCMS4B.html.
- [12] Patent RU2790949C1. URL: <https://patents.google.com/patent/RU2790949C1/ru>
- [13] V. Sokolov, I. Potemin, Y. Wang. Virtual prototyping of BSDF measurements for materials with complex scattering properties // Proceedings of SPIE - 2021, Vol. 11876, pp. 118760K.
- [14] V. Sokolov, I. Potemin, D. D. Zhdanov, B. Barladian. Simulation of the BSDF measurements for scattering materials with GP-200 gonio-photometer for light guiding plates // Proceedings of SPIE - 2021, Vol. 11783, pp. 1178305.
- [15] Xenon Arc Lamp, 150 W, Ozone Free, Newport, 2023. URL: <https://www.newport.com/p/6255>
- [16] Oriel mini monochromator, 2023. URL: https://research.engineering.ucdavis.edu/woodall/wp-content/uploads/sites/84/2016/02/oriel_78025_specs.pdf.
- [17] Lumicept – Hybrid Light Simulation Software, 2023. URL: <https://integra.jp/en/products/lumicept>.